



Visualizing medium and bio-distribution in complex cell culture bioreactors using in-vivo imaging

Journal:	<i>Biotechnology Progress</i>
Manuscript ID:	BTPR-13-0318.R1
Wiley - Manuscript type:	Notes
Date Submitted by the Author:	n/a
Complete List of Authors:	Ratcliffe, Elizabeth; Loughborough University, Wolfson School of Mechanical and Manufacturing Engineering Stacey, Adrian; TAP Biosystems, Thomas, Robert; Loughborough University, Wolfson School of Mechanical and Manufacturing Engineering
Keywords:	Cell culture, Bioreactor, Bio-distribution, Process development, 3d imaging

SCHOLARONE™
Manuscripts

view

1
2
3
4
5
6
7
8
9 **Visualizing medium and bio-distribution in complex cell culture**
10
11 **bioreactors using in-vivo imaging**
12
13

14
15 E. Ratcliffe^{a*}, A.J. Stacey^b, R.J. Thomas^a
16
17

18
19 *^aHealthcare Engineering Research Group, Centre for Biological Engineering, Wolfson*
20
21 *School of Mechanical and Manufacturing Engineering, Loughborough University,*
22
23 *Loughborough, Leicestershire, LE11 3TU, United Kingdom.*
24
25

26
27 *^bTAP Biosystems, York Way, Royston, Hertfordshire, SG8 5WY, United Kingdom.*
28
29
30
31
32

33 *Corresponding author: E. Ratcliffe, Healthcare Engineering Research Group, Centre for
34 Biological Engineering, Wolfson School of Mechanical and Manufacturing Engineering,
35 Loughborough University, Loughborough, LE11 3TU, United Kingdom. Telephone: +44-
36 1509-564889, Fax: +44-1509-227648, *E-mail address:* E.Ratcliffe@lboro.ac.uk
37
38
39
40
41
42
43
44
45
46
47
48
49
50
51
52
53
54
55
56
57
58
59
60

1
2
3 **Abstract.** There is a dearth of technology and methods to aid process characterization,
4
5 control and scale-up of complex culture platforms that provide niche micro-environments for
6
7 some stem cell-based products. We have demonstrated a novel use of 3d in-vivo imaging
8
9 systems to visualize medium flow and cell distribution within a complex culture platform
10
11 (hollow fiber bioreactor) to aid characterization of potential spatial heterogeneity and identify
12
13 potential routes of bioreactor failure or sources of variability. This can then aid process
14
15 characterization and control of such systems with a view to scale-up. Two potential sources
16
17 of variation were observed with multiple bioreactors repeatedly imaged using two different
18
19 imaging systems: shortcutting of medium between adjacent inlet and outlet ports with the
20
21 potential to create medium gradients within the bioreactor, and localization of bioluminescent
22
23 murine 4T1-*luc2* cells upon inoculation with the potential to create variable seeding densities
24
25 at different points within the cell growth chamber. The ability of the imaging technique to
26
27 identify these key operational bioreactor characteristics demonstrates an emerging technique
28
29 in troubleshooting and engineering optimization of bioreactor performance.
30
31
32
33
34
35
36
37
38
39
40
41
42
43
44
45
46
47
48
49
50
51
52
53
54
55
56
57
58
59
60

1
2
3 Stem cell-based products always incorporate some heterogeneity due to variability in
4 biological input materials, different micro-environments in the bioprocess and cell sensitivity
5 to extrinsic factors. Improving the understanding, characterization and control of a bioprocess,
6 is essential in ensuring process reproducibility and product quality¹⁻⁴. In-process
7 measurements aid process understanding and control, and one of the most commonly used
8 methods of in-process measurement is cell number and cell viability determination, but many
9 tests are invasive and subjective^{1, 5}. There is a requirement for improved process control
10 equipment and techniques, and the use of quantitative non-invasive and non-destructive
11 automated imaging techniques are expected to become more prevalent for on-line
12 monitoring⁶. However current techniques are primarily suited to 2-dimensional adherent cell
13 culture formats, and for many applications 3d culture is preferable for scalable manufacture⁷.
14 Although many 3d culture systems have on-line monitoring and culture maintenance
15 capabilities, and traditional 3d stirred tank production technology is known to perform and be
16 readily scalable for suspension cultures^{2, 8, 9}, more complex 3d platforms are required for
17 some cell-based bioprocesses in order to provide a more appropriate micro-environment^{9, 10}.
18 For example, perfused hollow fiber bioreactors have been used for primary human
19 hepatocytes¹¹ and hematopoietic progenitor cells¹², where the stem cell niche is considered of
20 critical importance to successful expansion, differentiation and maturation. An advantage of
21 these more complex perfused bioreactors is a higher surface area to volume ratio leading to
22 potentially higher product yields, improved homogeneity relative to fed-batch or static
23 methods, and reduced waste accumulation. Yet the disadvantages associated with such
24 systems are variable harvest yield, increased risk of heterogeneous culture conditions or cell
25 distribution with complex internal structure/flow (primarily rigid systems), increased risk of
26 problematic cell dissociation, and unknown or negative effects of continuous removal of
27 paracrine factors^{13, 6, 10}. There is a requirement to evaluate methods of in-process bioreactor
28
29
30
31
32
33
34
35
36
37
38
39
40
41
42
43
44
45
46
47
48
49
50
51
52
53
54
55
56
57
58
59
60

1
2
3 monitoring and bioreactor failure modes in such systems that are inherently difficult to
4
5 characterize in order to assess what drives variability in such systems. Here we demonstrate
6
7 the proof of principle that 3d in-vivo imaging systems can be utilized to image medium and
8
9 bio- distribution in a hollow fiber cell culture bioreactor to aid characterization of potential
10
11 spatial heterogeneity and sources of variability.
12
13

14
15 Two potential sources of heterogeneity were investigated: media distribution and cell
16
17 seed distribution within the bioreactor. Equipment for *in vivo* bio-monitoring were considered
18
19 as good candidates to allow monitoring of flow patterns and cell distribution in the bioreactor.
20
21 The laboratory scale bioreactor has an 8 mL cell chamber whereas the clinical scale
22
23 bioreactor has an 800 mL cell chamber (Stemcell Systems GmbH, Berlin, Germany). The cell
24
25 chamber comprises layers of counter-currently perfused medium capillaries with integrated
26
27 gas capillaries. Cells are cultured outside the fibers in the extra-capillary space and medium /
28
29 gas is circulated through semi-permeable fibers through the intra-capillary space. The internal
30
31 structure of the bioreactor, the perfusion set up, perfusion and inoculation conditions have
32
33 been described in detail elsewhere¹³. Two imaging systems were used; the Pearl Impulse
34
35 system (LI-COR Biosciences, Cambridge, UK) and the Ivis Kinetic system (Caliper Life
36
37 Sciences, Cheshire, UK). As the Pearl Impulse system does not have the chamber capacity to
38
39 analyze an 800 mL bioreactor, a further high capacity system, the Ivis Kinetic, was also
40
41 investigated as this has the potential for downstream use with a scaled bioreactor.
42
43
44
45

46
47 **Medium distribution.** The Pearl Impulse Imager was shown to be capable of detecting
48
49 artificially induced fluorescence and flow patterns of fluorescent liquid (IR Dye[®] 800CW
50
51 probe, LI-COR Biosciences) within the bioreactor and these signals were distinguishable
52
53 from background auto-fluorescence of the plastic. Fluorescent dye-spiked buffer was
54
55 perfused under counter-current flow through the bioreactor to capture video of flow
56
57 characteristics. Figure 1 shows a cross-section of still images from a representative video
58
59
60

1
2
3 sequence. It identifies shortcutting of medium flow from the inlet port to the adjacent exit
4 port, rather than crossing the bioreactor to the appropriate opposite exit port for each medium
5 capillary network. The medium shortcutting was observed at the higher flow 20 mL/min
6 medium recirculation rate¹³ and could potentially decrease the homogeneity of the bioreactor
7 and linearity of process scalability. As perfusion continued for a few minutes medium was
8 subsequently capable of circulating to all parts of the chamber at this flow rate (as shown in
9 the latter images from the video sequence). Prior to using the Ivis Kinetic imager, spectral
10 analysis of the hollow fiber bioreactor was conducted using an Ivis Spectrum system (Caliper
11 Life Sciences) to image the bioreactor with a large number of filters (green fluorescent
12 protein, GFP, range to near-infrared, NIR, range) to identify excitation/emission
13 combinations for the lowest background noise signal. The 710/780 excitation/emission filter
14 combination provided the lowest background fluorescence, indicating the Xenolight CF750
15 dye (Caliper Life Sciences) or similar alternative and the 700 nanometer (nm) filter wheel in
16 the Ivis Kinetic would achieve the best fluorescent imaging data (Figure 2A). Additionally,
17 Figure 2B, with blocked excitation, showed that the bioreactor had no detectable
18 phosphorescence suggesting the possibility of tracking a bioluminescent cell population. The
19 shortcutting of fluorescent dye-spiked media between adjacent medium in-flow and out-flow
20 ports observed previously was also observed when bioreactors were imaged using the Ivis
21 Kinetic under identical counter-current medium perfusion conditions (Figure 2C shows a still
22 image from a representative video sequence). The effect of medium short-cutting was
23 observed in multiple bioreactors with two different imaging systems suggesting that this
24 could be a source of potential process variation. Additionally, as medium short-cutting was
25 observed at the higher circulation flow rate, there is potential for differences or gradients to
26 arise at lower flow rates such as the 4 mL/min cell feeding rate¹³.

27
28
29
30
31
32
33
34
35
36
37
38
39
40
41
42
43
44
45
46
47
48
49
50
51
52
53
54
55
56
57
58
59
60

1
2
3 **Cell Seeding distribution.** A mock cell seeding exercise using the Pearl Impulse Imager and
4 inoculating fluorescent dye-spiked buffer (IR Dye[®] 800CW, 800 nm fluorescence channel)
5 into the cell inoculation port appeared to show uneven dye distribution after seeding, thereby
6 suggesting the potential for non-homogenous cell density within the cell chamber as another
7 possible candidate for introducing process variability. To further investigate cell distribution
8 after seeding into the cell chamber of the bioreactor, a population of bioluminescent murine
9 cells (4T1-*luc2*, Caliper Life Sciences) were inoculated into the bioreactor under conditions
10 described previously¹³. The Ivis Kinetic imager was able to detect the bioluminescent
11 population within the hollow fiber bioreactor, and showed that the cells appeared to localize
12 in the center of the cell chamber (Figure 3), suggesting that distribution in the compartment
13 may not be homogenous at inoculation.
14
15
16
17
18
19
20
21
22
23
24
25
26
27
28

29 Shortcutting of medium between adjacent inlet and outlet ports has the potential to
30 create medium gradients, and heterogeneous distribution of cells upon inoculation has the
31 potential to create variable seeding densities within the bioreactor. Such sources of variation
32 could cause considerable process performance heterogeneity problems with scale-up. Small
33 scale bioreactor systems using low cell densities tend to function well as there is an excess of
34 nutrients available. However, as systems are scaled and higher cell densities achieved, early
35 identification of heterogeneity issues can be critical as cell and medium gradients may result
36 in some cells being starved of both nutrients and oxygen with others being overfed. Variation
37 in harvest cell yield from the bioreactors has been observed previously¹³ and the ability of the
38 imaging technique to identify these key operational bioreactor characteristics that may
39 contribute to such variation demonstrates a powerful emerging role in troubleshooting and
40 engineering optimization of bioreactor performance. Defining procedures to maximize cell
41 seeding homogeneity (e.g. optimized liquid chasing or bioreactor rotation procedures) could
42
43
44
45
46
47
48
49
50
51
52
53
54
55
56
57
58
59
60

1
2
3 improve this situation and be further explored with imaging as an initial output, with
4
5 subsequent population distribution tracking, cell yield, viability and characterization
6
7 measurements. Imaging could also be used as an initial output alongside cell yield and
8
9 viability to further inform modeling experiments and explore the effect of optimizing medium
10
11 perfusion rates and distribution on cell expansion or other bioreactor phenomena such as
12
13 Starling flows (secondary flow in the cell chamber driven by elevated medium recirculation
14
15 levels in the capillaries)^{14, 15}. Technique limitations would also need to be further defined, for
16
17 example the qualitative nature of the 2d heat-map data may be addressed by region of interest
18
19 (ROI) definition to attain quantitative fluorescence and phosphorescence data from the
20
21 Imaging system software. As well as further definition of the potential for obtaining complete
22
23 3d images and quantitative data. More work is also required to define the achievable
24
25 resolution of the technique, for example whether single cell imaging is possible.
26
27
28
29
30

31
32 The technique may also be useful for other hollow fiber technology applications. For
33
34 example, Pinzon *et al.* (2013) recently demonstrated a microbe-based bio-surfactant
35
36 production process using hollow fiber technology under denitrifying conditions in order to
37
38 eliminate the common oxygen transfer limitations and foaming difficulties that are inherent to
39
40 the current aerobic process¹⁶. Cell entrapment within the extra-capillary space offered the
41
42 advantage of easy soluble product recovery from perfused medium and the authors suggest
43
44 bioreactor scale-up should be explored¹⁶. The imaging technique described may offer
45
46 advantages to the scaling process to assess labeled cell distribution or tracing labeled
47
48 feedstock compounds for localization or limitation. Additionally as continuous product
49
50 harvesting via multivalent cation addition and extraction is an attractive concept¹⁶ the
51
52 technique could be used to assess residues alongside cell tracking and measures of cell
53
54 viability. Another area where the technique may offer unique advantages is for those
55
56
57
58
59
60

1
2
3 processes that require further cell immobilization, for example alginate immobilization to
4
5 promote stem cell differentiation or increased levels of insulin production in pancreatic /
6
7 islet-like cell clusters¹⁷. A novel bioprocess for alginate immobilization of mammalian cells
8
9 within a hollow-fiber bioreactor was recently demonstrated by Hoesli *et al.* (2009) and key
10
11 processing issues included the obstruction of medium flow due to alginate crossing the
12
13 membranes from the extra-capillary space into the intra-capillary space as well as cell
14
15 recovery from the extra-capillary space¹⁷. The method used to assess effective alginate
16
17 gelling during method development was visual inspection of sawed hollow fiber cartridges¹⁷.
18
19 The imaging technique described would eliminate the need for destruction of hollow fiber
20
21 cartridges and could be used to trace labeled alginate for effective gelling or labeled medium
22
23 flows through alginate bioreactors. Additionally, labeled cells could be used for method
24
25 development of cell recovery or to trace effective removal and residues of temperature
26
27 sensitive alginate gel for more effective recovery.
28
29
30
31
32
33

34 The work described demonstrates that as a proof-of-principle medium and bio-
35
36 distribution imaging in complex hollow fiber cell culture bioreactors is possible using 3d in-
37
38 vivo imaging techniques. Additionally, imaging of medium distribution and bioluminescent
39
40 cell populations in this manner could be particularly useful for early detection of
41
42 heterogeneity within complex 3d cell culture platforms and aid engineering of operational
43
44 parameters to improve process performance and control prior to scale-up.
45
46
47
48

49 **Materials and Methods.** The Pearl Impulse system is a fluorescent imaging platform with
50
51 laser excitation and near-infrared (NIR) fluorescence detection (see
52
53 http://www.licor.com/bio/products/imaging_systems/pearl/pearl_imager.jsp). The Ivis
54
55 Kinetic system is a filter-based platform for fluorescence (green fluorescent protein, GFP-
56
57 NIR range) or bio-luminescence (see
58
59
60

1
2
3 www.perkinelmer.com/SG/Catalog/Category/ID/IVIS%20Series). The hollow fiber
4
5 bioreactors were provided courtesy of Celgene Cellular Therapeutics (New Jersey, USA);
6
7 they are produced by Stemcell Systems GmbH (Berlin, Germany)^{13, 18}. Each laboratory scale
8
9 bioreactor consists of an 8 mL cell compartment and multiple layers of three independent
10
11 capillary networks that are interwoven and provide counter-current medium perfusion and
12
13 integrated gas supply. The internal structure of the bioreactor, the perfusion set up, perfusion
14
15 and inoculation conditions have been described in detail elsewhere¹³. Bioreactors were
16
17 perfused at the medium recirculation rate of 20 mL/min¹³. Fluorescent imaging of liquid flow
18
19 patterns with the Pearl Impulse imager (calibrated to manufacturer's standards) was
20
21 performed using the IR Dye[®] 800CW probe (1 µg/mL in PBS, LI-COR Biosciences), 800
22
23 nanometers (nm) fluorescence channel detection and 0.5 s image acquisition. Spectral
24
25 analysis of the bioreactor was performed using an Ivis Spectrum imaging platform (Caliper
26
27 Life Sciences, calibrated to manufacturer's standards) to image the bioreactor rapidly with
28
29 GFP range to NIR range filters for background fluorescence as well as phosphorescence.
30
31 Fluorescent imaging of liquid flow patterns with the Ivis Kinetic imager (calibrated to
32
33 manufacturer's standards) was performed using the Xenolight CF750 dye (1 mM in dH₂O),
34
35 700 nm filter wheel detection and 0.5 s image acquisition. Cell localization imaging was
36
37 performed using the luciferase expressing 4T1-*luc2* Bioware Ultra murine cell line, cultured
38
39 according to manufacturer's conditions in RPMI-1640 medium (ATCC, #30-2001)
40
41 supplemented with 10% FBS (Fisher Scientific, Loughborough, UK). 4T1-*luc2* cells were
42
43 prepared to 5×10⁴/mL density and exposed to Xenolight D-luciferin potassium salt substrate
44
45 (150 µg/mL in RPMI-1640) at 37°C for 5 min. Cells were inoculated into the 8 mL bioreactor
46
47 cell chamber port at a density of 8×10⁵/mL (6.4×10⁶ cells in total), as described previously¹³,
48
49 for subsequent imaging (37 °C imaging chamber). All reagents, cell lines and substrates for
50
51 Ivis Kinetic Imaging were provided courtesy of Caliper Life Sciences. Imaging was
52
53
54
55
56
57
58
59
60

1
2
3 performed in duplicate (minimum) with duplicate (minimum) bioreactors unless otherwise
4
5 stated, a total of 6 bioreactors were used in this study.
6
7

8 **Acknowledgements.** This work was funded by Celgene Cellular Therapeutics via the US
9
10 Defense Advanced Research Projects Agency (DARPA) and the Defense Sciences Office
11
12 (DSO) Blood Pharming program (Grant number FA9550-08-1-0392). We are grateful for the
13
14 discussions, excellent technical support and photographs from Dr Kevin Francis, Dr Tim
15
16 Devling, JaeBeom Kim, Ken Wong and Jay Whalen (Caliper Life Sciences, PerkinElmer);
17
18 and Dr Geoff Dance (LI-COR Biosciences)
19
20
21

22 **References**

- 23
24
25 1. Lim M, Ye H, Panoskaltis N, Drakakis EM, Yue X, Cass AE, Radomska A,
26
27 Mantalaris A. Intelligent bioprocessing for hematopoietic cell cultures using
28
29 monitoring and design of experiments. *Biotechnol Adv.* 2007; 25: 353-368.
30
31
- 32
33 2. Kirouac D, Zandstra P. The systematic production of cells for cell therapies. *Cell Stem*
34
35 *Cell.* 2008; 3: 369-381.
36
- 37
38 3. Placzek M, Chung I, Macedo H, Ismail S, Mortera Blanco T, Lim M, Cha J, Fauzi I,
39
40 Kang Y, Yeo D, Ma C, Polak J, Panoskaltis N, Mantalaris A. Stem cell
41
42 bioprocessing: fundamentals and principles. *J R Soc Interface.* 2009; 6: 209-232.
43
44
- 45
46 4. Williams D, Thomas R, Hourd P, Chandra A, Ratcliffe E, Liu Y, Rayment E, Archer
47
48 J. Precision manufacturing for clinical-quality regenerative medicines. *Philos*
49
50 *Transact A Math Phys Eng Sci* 2012; 370(1973): 3924-3949.
51
- 52
53 5. Berridge M, Tan A. Characterization of the cellular reduction of 3-(4, 5-
54
55 dimethylthiazol-2-yl)-2, 5-diphenyltetrazolium bromide (MTT): Subcellular
56
57 localization, substrate dependence, and involvement of mitochondrial electron
58
59 transport in Mtt reduction. *Arch Biochem Biophys.* 1993; 303: 474-482.
60

- 1
2
3 6. Ratcliffe E, Thomas RJ, Williams DJ. Current understanding and challenges in
4
5 bioprocessing of stem cell-based therapies for regenerative medicine. *Br Med Bulletin*.
6
7 2011; 100: 137–155.
- 8
9
10 7. Liu Y, Liu T, Fan X, Ma X, Cui Z. Ex vivo expansion of hematopoietic stem cells
11
12 derived from umbilical cord blood in rotating wall vessel. *J Biotechnol*. 2006; 124:
13
14 592-601.
- 15
16 8. Nielsen L. Bioreactors for hematopoietic cell culture. *Annu Rev Biomed Eng*. 1999;
17
18 1(1523-9829): 129-152.
- 19
20 9. Cabrita G, Ferreira B, Lobato da Silva C, Gonçalves R, Almeida-Porada G, Cabral J.
21
22 Hematopoietic stem cells: from the bone to the bioreactor. *Trends Biotechnol*. 2003;
23
24 21(5): 233-240.
- 25
26
27 10. Thomson H. Bioprocessing of embryonic stem cells for drug discovery. *Trends*
28
29 *Biotechnol*. 2007; 25(5): 224-230.
- 30
31
32 11. Zeilinger K, Schreiter T, Darnell M, Söderdahl T, Lübberstedt M, Dillner B,
33
34 Knobeloch D, Nüssler A, Gerlach J, Andersson T. Scaling down of a clinical three-
35
36 dimensional perfusion multi-compartment hollow fiber liver bioreactor developed for
37
38 extracorporeal liver support to an analytical scale device useful for hepatic
39
40 pharmacological in vitro studies. *Tissue Eng Part C*. 2011; 17(5): 549 – 556.
- 41
42
43 12. Sardonini C, Wu Y. Expansion and differentiation of human hematopoietic cells from
44
45 static cultures through small-scale bioreactors. *Biotechnol Prog*. 1993; 9(2): 131-137.
- 46
47
48 13. Houssler G, Miki T, Schmelzer E, Pekor C, Zhang X, Kang L, Voskinarian-Berse V,
49
50 Abbot S, Zeilinger K, Gerlach J. Compartmental hollow fiber capillary membrane–
51
52 based bioreactor technology for in vitro studies on red blood cell lineage direction of
53
54 hematopoietic stem cells. *Tissue Eng Part C* 2012; 18(2): 133-142.
- 55
56
57
58
59
60

- 1
2
3 14. Starling E.H. On the absorption of fluid from the connective tissue spaces. *J Physiol*
4
5 (Lond) 1896; 19: 312-326.
6
7 15. Gramer M, Poeschl D, Conroy M, Hammer B. Effect of harvesting protocol on
8
9 performance of a hollow fiber bioreactor. *Biotechnol Bioeng*. 2000; 65(3): 334-340.
10
11 16. Pinzon N, Cook A, Ju L-K. Continuous rhamnolipid production using denitrifying
12
13 *Pseudomonas aeruginosa* cells in hollow-fiber bioreactor. *Biotechnol Prog*. 2013;
14
15 29(2): 352-358.
16
17 17. Hoesli C, Luu M, Piret J. A novel alginate hollow fiber bioreactor process for cellular
18
19 therapy applications. *Biotechnol Prog*. 2009; 25(6): 1740-1751.
20
21 18. Schmelzer E, Mutig K, Schrade P, Bachmann S, Gerlach J, Zeilinger K. Effect of
22
23 human patient plasma ex vivo treatment on gene expression and progenitor cell
24
25 activation of primary human liver cells in multi-compartment 3d perfusion bioreactors
26
27 for extra-corporeal liver support. *Biotechnol Bioeng*. 2009; 103(4): 817-827.
28
29
30
31

Figure Captions

32
33 **Figure 1.** Image A shows the hollow fiber bioreactor structure: (Port 1) gas outlet, (2)
34
35 medium outlet, (3) counter-current flow medium inlet, (4) cell inoculation port, (5) gas inlet,
36
37 (6) medium inlet and (7) medium outlet. Inset: illustrated hollow fiber layers of gassing
38
39 (grey), medium (pink), and counter-current flow medium (blue) fibers. Image B shows a
40
41 cross-section of still images from a representative video sequence of counter-current flow
42
43 medium perfusion. The images were taken using the Pearl Impulse Imaging system, IR Dye[®]
44
45 800CW and the 800 nm fluorescence channel. Numbered bioreactor ports (1-7) are clearly
46
47 visible at the beginning of the sequence (B1) and the bioreactor remains in the same
48
49 orientation throughout imaging. White arrows show counter-current medium perfusion (B1)
50
51 and black arrows show medium short-cutting to adjacent rather than opposite exit ports (B4).
52
53
54
55
56
57
58
59
60

1
2
3 **Figure 2.** Spectral analysis of the hollow fiber bioreactor using an Ivis Spectrum imaging
4 system and GFP to NIR range filters. Bioreactor ports are numbered from 1-7 (in white) to
5 show orientation (black port numbers painted on the bioreactor casing have been obscured by
6 signal in some places). Image A shows the minimal background noise signal can be achieved
7 with the 710/780 excitation/emission filter combination. Image B shows blocked excitation
8 and no detectable phosphorescence for bioluminescence experimentation. Image C is taken
9 from a video sequence using the Ivis Kinetic Imaging system (710/780 excitation/emission
10 filter combination) and shows Xenolight CF750 fluorescent dye-spiked counter-current
11 medium perfusion (white arrows) and medium short cutting to adjacent rather than opposite
12 exit ports (black arrows).
13
14
15
16
17
18
19
20
21
22
23
24
25

26 **Figure 3.** Ivis Kinetic Imager photographs of the bioreactor from two angles after inoculation
27 of luciferase expressing 4T1-*luc2* Bioware Ultra murine cells (6.4×10^6 cells at 8×10^5 /mL
28 density) into the cell chamber to assess inoculated cell distribution. Bioreactor ports are
29 numbered from 1-7 (in white) to show orientation (black port numbers painted on the
30 bioreactor casing have been obscured by signal in some places). Port 4 is used for cell
31 inoculation into the cell chamber.
32
33
34
35
36
37
38
39
40
41
42
43
44
45
46
47
48
49
50
51
52
53
54
55
56
57
58
59
60

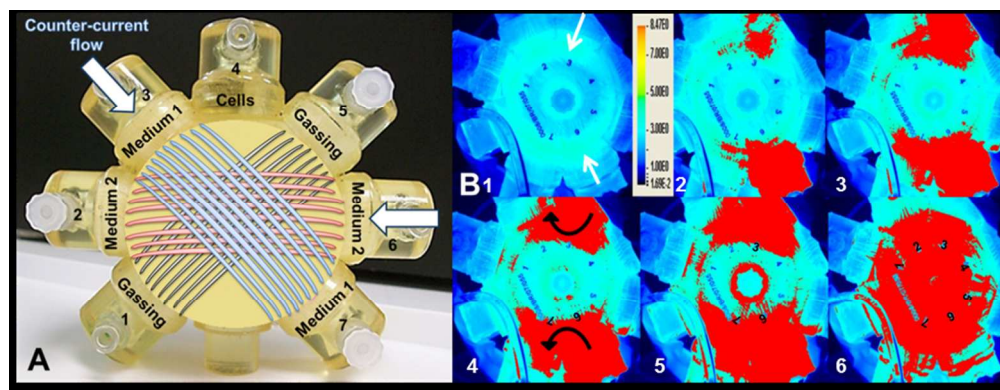
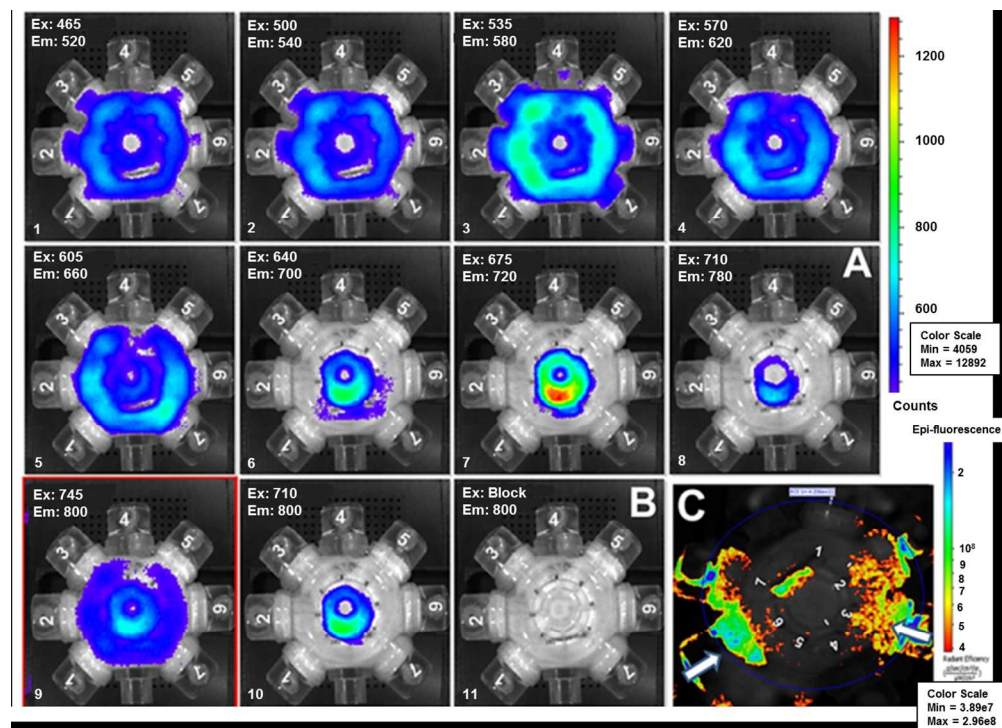


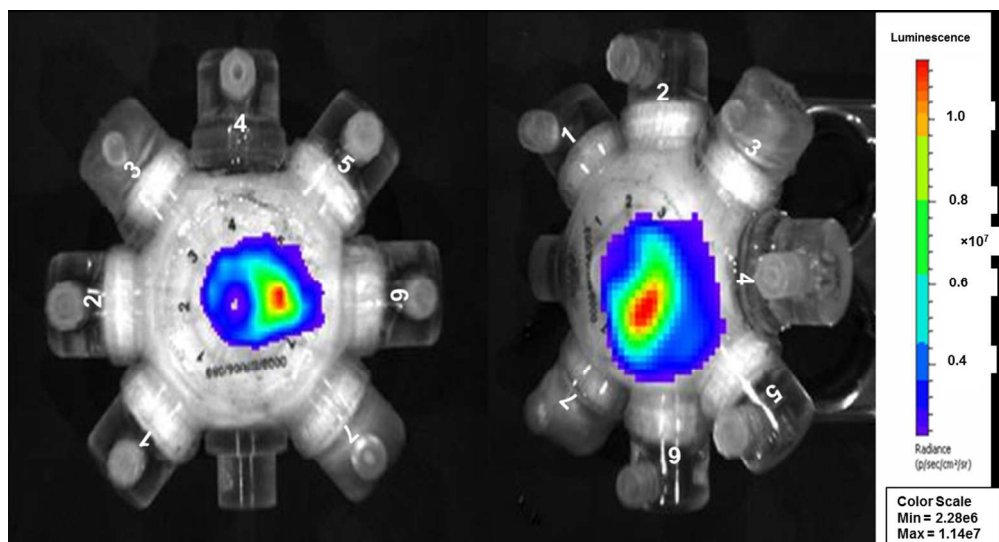
Image A shows the hollow fiber bioreactor structure: (Port 1) gas outlet, (2) medium outlet, (3) counter-current flow medium inlet, (4) cell inoculation port, (5) gas inlet, (6) medium inlet and (7) medium outlet.

Inset: illustrated hollow fiber layers of gassing (grey), medium (pink), and counter-current flow medium (blue) fibers. Image B shows a cross-section of still images from a representative video sequence of counter-current flow medium perfusion. The images were taken using the Pearl Impulse Imaging system, IR Dye® 800CW and the 800 nm fluorescence channel. Numbered bioreactor ports (1-7) are clearly visible at the beginning of the sequence (B1) and the bioreactor remains in the same orientation throughout imaging. White arrows show counter-current medium perfusion (B1) and black arrows show medium short-cutting to adjacent rather than opposite exit ports (B4).

88x34mm (300 x 300 DPI)



Spectral analysis of the hollow fiber bioreactor using an Ivis Spectrum imaging system and GFP to NIR range filters. Bioreactor ports are numbered from 1-7 (in white) to show orientation (black port numbers painted on the bioreactor casing have been obscured by signal in some places). Image A shows the minimal background noise signal can be achieved with the 710/780 excitation/emission filter combination. Image B shows blocked excitation and no detectable phosphorescence for bioluminescence experimentation. Image C is taken from a video sequence using the Ivis Kinetic Imaging system (710/780 excitation/emission filter combination) and shows Xenolight CF750 fluorescent dye-spiked counter-current medium perfusion (white arrows) and medium short cutting to adjacent rather than opposite exit ports (black arrows).
125x90mm (300 x 300 DPI)



Ivis Kinetic Imager photographs of the bioreactor from two angles after inoculation of luciferase expressing 4T1-*luc2* Bioware Ultra murine cells (6.4×10^6 cells at 8×10^5 /mL density) into the cell chamber to assess inoculated cell distribution. Bioreactor ports are numbered from 1-7 (in white) to show orientation (black port numbers painted on the bioreactor casing have been obscured by signal in some places). Port 4 is used for cell inoculation into the cell chamber.

119x64mm (300 x 300 DPI)